

Supercomputer Analysis of Sedimentary Basins

CRAIG M. BETHKE, WENDY J. HARRISON, CRAIG UPSON, STEPHEN P. ALTANER

Geological processes of fluid transport and chemical reaction in sedimentary basins have formed many of the earth's energy and mineral resources. These processes can be analyzed on natural time and distance scales with the use of supercomputers. Numerical experiments are presented that give insights to the factors controlling subsurface pressures, temperatures, and reactions; the origin of ores; and the distribution and quality of hydrocarbon reservoirs. The results show that numerical analysis combined with stratigraphic, sea level, and plate tectonic histories provides a powerful tool for studying the evolution of sedimentary basins over geologic time.

ALTHOUGH SEDIMENTARY BASINS HOLD MANY OF THE earth's economic resources, including nearly all reservoirs of petroleum and natural gas and various ores, much remains to be learned about the processes that shape the subsurface. Basins are areas of the earth's surface that downwarpage and accept sediments and pore fluids over geologic time. Sediments are transported into basins by stream, ocean, and atmospheric currents or are precipitated directly or biologically from seawater. As sediments are buried, they compact, warm to temperatures as high as 300°C by heat conducted from the lower crust, and lithify to form sedimentary rocks. Pore fluids at depth become laden with salts and dissolved minerals. As sediments encounter higher temperatures and pressures and react with subsurface fluids, they alter chemically and physically by processes collectively referred to as diagenesis. When minerals are removed from surface conditions, they transform, dissolve, or react with pore fluids and each other to form new assemblages; other minerals precipitate from ground waters to form cements in pore spaces. Compaction and cementation seal some rocks, but many remain highly permeable so that fluids can circulate and redistribute heat and dissolved mass.

Economic resources form in the subsurface over geologic time. Organic matter buried with fine-grained sediments reacts to form hydrocarbons. After being expelled from source rocks, hydrocarbons migrate through carrier beds to traps where they accumulate into petroleum reservoirs. Reservoirs may form in rocks that resisted compaction because of early cements or high pore pressures, or that developed new pore space as minerals dissolved or transformed. Oxidizing surface waters, which dissolve uranium and other elements as they infiltrate basins, form ore deposits as they encounter reducing conditions at depth. Hot brines concentrate trace metals from deep sediments and then precipitate ore minerals as they cool.

C. M. Bethke and S. P. Altaner are in the Department of Geology, University of Illinois, Urbana, IL 61801. W. J. Harrison is at Exxon Production Research Company, Houston, TX 77001. C. Upson is at the National Center for Supercomputing Applications, Urbana, IL 61801.

Despite the economic and scientific importance of sedimentary basins, little is known about either the microscopic mechanisms or basinwide systematics of reaction and transport in the subsurface. Study of the sedimentary environment is complicated by the rates at which many processes occur. Sediments generally accumulate in basins at fractions of millimeters per year, and fluids may move only centimeters per year. These rates are significant; a fluid that moves 1 cm/year over the 500-million-year history of the interior basins of North America would traverse 5000 km. Most basin studies have centered on either direct observation or laboratory simulation. Such studies give considerable insight, but observations can be made only at an instant in geologic time, and laboratory experiments are difficult to extrapolate to natural time and distance scales.

Supercomputer Analysis

Supercomputer simulation can complement these studies. Supercomputers have large memories and use special architectures to perform calculations rapidly. These computers can simulate more complicated processes than conventional machines or allow a researcher to evaluate quickly the effects of a variety of scenarios on the evolution of a system of interest. In the latter case, the researcher gains an intuitive feel for the behavior of the system being studied. In basin analysis, the chemical and physical relations describing motion and reaction of fluids and sediment are integrated with data from field and laboratory studies to evaluate the evolution of subsurface processes quantitatively. This type of simulation provides the only method available for studying sedimentary basins on natural time and distance scales.

Evaluating the governing equations is commonly impractical without especially rapid computers because of the complexity of the subsurface and the long time spans considered in geologic problems. Most supercomputers rely on fast instruction cycling and an accel-

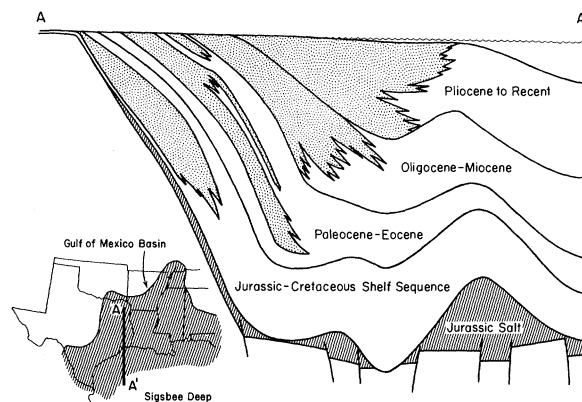
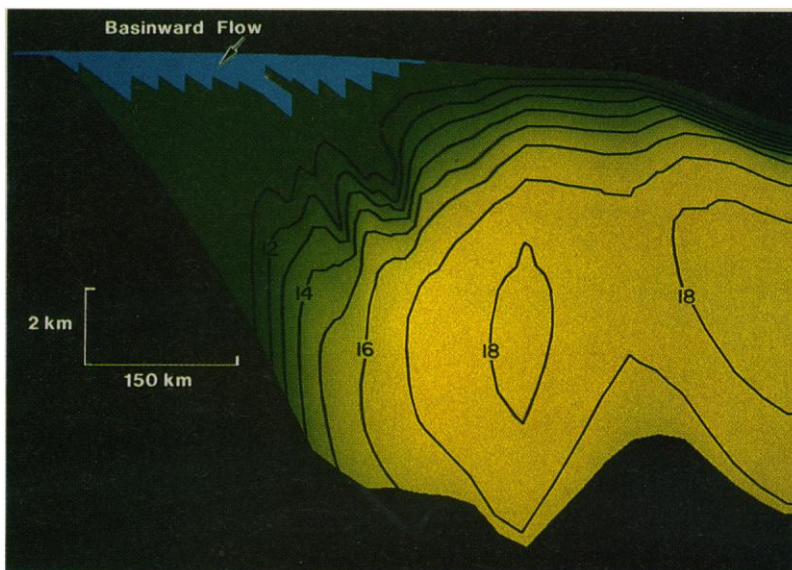


Fig. 1. Gulf of Mexico basin and north-south geologic cross section.

Fig. 2. Calculated present-day distribution of geopressures in the Gulf basin. Vertical exaggeration is 40:1. Contours and color shading show pressure gradient (in megapascals per kilometer). Gradients in excess of 16 MPa/km represent hard geopressures. The blue area shows the extent of basinward flow due to topographic relief on the coastal plain.



eration technique known as vectorization. These vector computers are expensive to manufacture and maintain because cycle speeds approach perceived physical limits of semiconductor technology. We obtained the results in this article by using a computer with a novel parallel-vector architecture (1). This computer contains six inexpensive vector processors that share a common memory. The processors operating in parallel compute our hydrologic models of basin evolution at 70% of the speed of the vector processor of a current generation supercomputer, but at a fraction of the cost. To our knowledge these are among the first published applications of a parallel-vector computer.

Gulf Coast Geopressures

The Gulf of Mexico basin, the richest petroleum province in North America, is characterized by widespread areas where pore fluid pressures are much greater than the hydrostatic pressures normally encountered in the subsurface. Geopressured fluids blow out oil wells during drilling, which poses a critical problem in petroleum exploration. Over geologic time, geopressures play inferred roles in forming growth faults, localizing petroleum reservoirs, and creating metallic ores; geopressured fluids may provide a resource of thermal and mechanical energy.

The Gulf basin formed when the North and South American plates rifted apart, a process that began in the Triassic (2). In the Triassic and Jurassic, clastic sediments and thick salt beds covered basement rocks of continental and oceanic crust. The evaporites later deformed under the weight of overlying sediments to form the salt domes widespread in the Gulf. These strata were overlain in the Jurassic and Cretaceous by clastic and carbonate sediments typical of a continental shelf. Since the beginning of the Tertiary, the basin has subsided rapidly and has been filled with sediments transported by the Mississippi and Rio Grande river systems. The sediments form deltaic wedges that prograde basinward.

Although nearshore sections contain sandy facies, much of the Tertiary sediments, especially in offshore sections, are clays that form thick, impermeable shale sequences. Geopressures develop because the impermeable sediments cannot expel fluids quickly enough to compact fully during burial (3). Geopressured zones occur at depths greater than about 2 to 3 km, and at somewhat shallower depths in offshore sections, over much of the Texas and Louisiana Gulf Coast. Subsurface pressures are described by the ratio of pressure to depth.

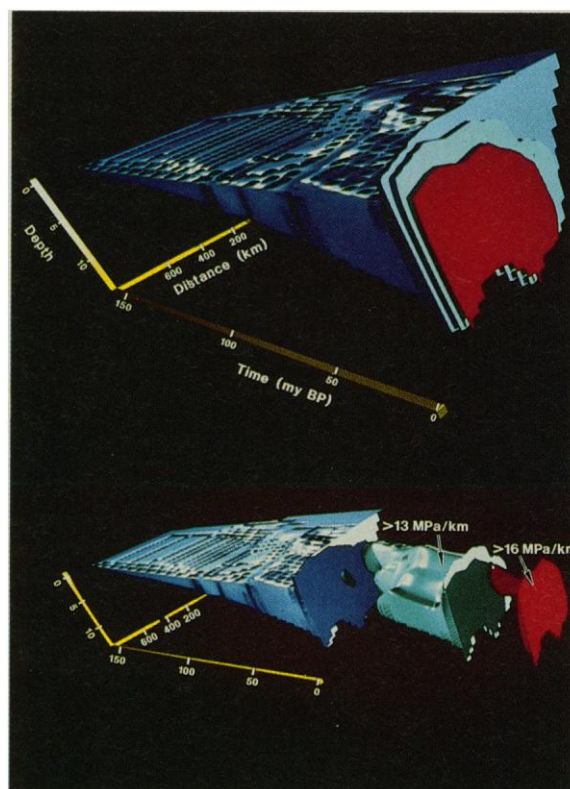


Fig. 3. Three-dimensional rendering of calculated geopressure development in the Gulf basin through geologic time. Perspective is from Sigsbee escarpment (south) looking landward. (Top) Basin subsidence and sedimentation from Jurassic to present and current distribution of pressure gradient. (Bottom) Exploded view showing the development of zones with pressure gradients greater than 13 and 16 MPa/km.

Gradients greater than 10 MPa/km (1 MPa \approx 10 atm) are overpressured, and those greater than 16 MPa/km describe hard geopressures.

We simulated the development of Gulf Coast geopressures through geologic time (4). Our calculation accounts for subsidence and filling of the basin, compaction of sediments during burial, and subsurface movement of pore fluids (5). In the simulation, the fluid pressure distribution $P(x,z,t)$, where x , z , and t are lateral position,

depth, and time, respectively, is found by solving an equation of flow through a deforming medium

$$\phi\beta \frac{\partial P}{\partial t} = \frac{\partial}{\partial x} \left[\frac{k_x}{\mu} \left(\frac{\partial P}{\partial x} \right) \right] + \frac{\partial}{\partial z} \left[\frac{k_z}{\mu} \left(\frac{\partial P}{\partial z} - \rho g \right) \right] - \frac{1}{(1-\phi)} \frac{\partial \phi}{\partial t} + \phi\alpha \frac{\partial T}{\partial t} \quad (1)$$

as an initial-boundary value problem. In Eq. 1, ϕ is porosity, α and β are, respectively, the thermal expansivity and compressibility of the pore fluid, k_x and k_z are directional permeabilities, μ is fluid viscosity, T is temperature, ρ is density of the pore fluid, and g is the acceleration of gravity. Porosity varies with effective stress, which is the difference between the stress exerted by the weight of overlying sediments and the fluid pressure. Temperature follows a conductive gradient with sediment burial. The top boundary, which moves to accept sedimentation, remains at hydrostatic pressure subsea and atmospheric pressure above sea level; other boundaries are barriers to flow. The calculation follows a cross section (Fig. 1) that runs approximately north-south through east Texas and extends 730 km from the landward extent of Jurassic outcrop to the offshore Sigsbee escarpment. The simulation begins with the deposition of the sediments covering the Jurassic evaporites and continues to the present, spanning 156 million years.

Calculation results for the present day show widespread geopressures in deep strata (Fig. 2) that closely reproduce known regional pressure distributions (6). Computed gradients vary from hydrostatic pressures to greater than 18 MPa/km, but do not reach the lithostatic gradient of 23 MPa/km, which is the theoretical limit at which pore fluids support the full weight of the overburden. In

nearshore sections, an abrupt transition from hydrostatically pressured to geopressed sediments occurs where sandy facies overlie shaly strata. Farther offshore, where sediments are more than 90% shale, geopressures develop in shallower sediments and gradually increase with depth. Success in matching the present-day pressure distribution in the Gulf suggests that past subsurface pressures can be estimated by numerical simulation and that pressures in frontier basins can be predicted before drilling.

The Gulf Coast is a well-known example of an overpressured basin, but the simulation indicates that widespread geopressures developed only in the past 2 million years (Fig. 3). For nearly all of the basin's 160-million-year history, pressures in most sediments remained near hydrostatic. From the Eocene to the Pliocene, a band of overpressures developed beneath the active depocenters. This information helps predict where reservoirs formed in the early Tertiary because petroleum tends to accumulate along the tops of geopressed zones (7). In the Plio-Pleistocene, geopressures expanded rapidly into strata that were previously near hydrostatic values, reaching their greatest intensity and distribution in the present day. The current widespread geopressures result from steady increase in sedimentation rates since the Miocene, apparently in response to uplift and erosion of the Colorado Plateau and generally low stands of sea level (8).

Midcontinent Brine Migrations

Warm brines migrated hundreds of kilometers through the sedimentary cover of the North American midcontinent in the geologic past. As the brines moved from depth into shallow sediments on the arches separating basins, they precipitated ore minerals to form the lead, zinc, barium, and fluorine resources of the Mississippi Valley (9). The ores lie in shallow strata that are cool today, but analysis of the ores shows that they formed from warm brines, mostly between 75° and 150°C. The migrating brines have

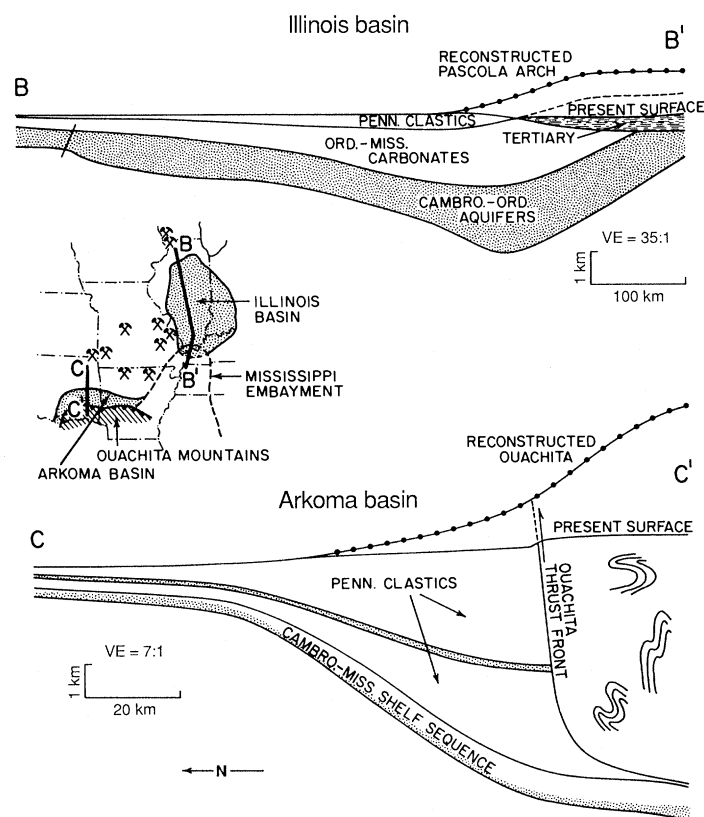


Fig. 4. North-south cross sections of Illinois and Arkoma basins showing reconstructed topography of Pascola arch and ancient Ouachita Mountains. Map shows distribution of major Mississippi Valley ores (crossed hammer and pick). VE, vertical exaggeration.

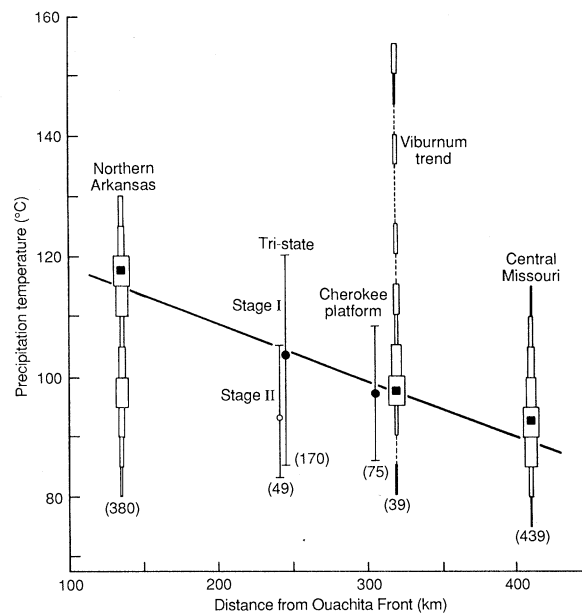


Fig. 5. Precipitation temperatures of sphalerite from the midcontinent plotted against distance from Ouachita Front, from analysis of fluid inclusions. Width of bars is proportional to number of measurements for each temperature range; the number of data points is shown in parentheses. Mineralization temperatures decrease systematically northward. The slope of the line represents a lateral temperature gradient of 0.09°C per kilometer. Squares show the mode of temperature determination; circles show the mean.

also redistributed hydrocarbons over remarkable distances. Correlating oils with their source rocks shows that transport occurred over distances greater than 150 km in the Williston (10) and Denver (11) basins, and the occurrence of long migrations have been inferred in the Alberta (12), Illinois (13), Anadarko, and Appalachian basins (14). Brine migrations have been variously ascribed to the compaction of basin sediments (15), decompression of geopressed zones (16), lateral compression of sediments during continental collisions (14), and topographic relief from tectonic uplift (17). Understanding the origin of the migrations is vital to efficient exploration for oil and minerals.

We modeled past ground-water flow and heat transport in the Illinois and Arkoma basins as initial-boundary value problems. The Illinois basin subsided from late Cambrian into at least Pennsylvanian time and accumulated more than 4 km of sediments on a crystalline basement (Fig. 4). Cambrian and early Ordovician strata are poor in shales but rich in permeable sandstones that form a basal aquifer complex. Ancient trade winds apparently winnowed clays from barren sediments before the evolution of land plants, which accounts for the high permeability of these strata (18). A late Ordovician through Mississippian interval of dominantly carbonate rocks overlies the basal system. The basin is capped by Pennsylvanian cyclothem of alternating sandstone, shale, carbonate, and coal. In the Mesozoic, uplift of the Pascola arch elevated sediments in the southern end of the basin. The arch has subsided and is buried today beneath the sediments of the Mississippi embayment. The Arkoma basin formed on a continental platform much like the Cambrian-Mississippian system in the Illinois basin. The basal formation is the Lamotte sandstone, a widespread aquifer. Collision of the North and South American plates uplifted the Ouachita Mountains in the Pennsylvanian. The craton adjacent to the mountains downwarped, which allowed rapid accumulation of more than 6 km of fine-grained sediments.

Our calculations solve an equation that describes heat transport by conduction and ground-water advection (5)

$$\left[\rho\phi C_w + \rho_r(1 - \phi)C_r \right] \frac{\partial T}{\partial t} = \nabla \cdot K\nabla T - \rho C_w \nabla \cdot (\mathbf{q}T) - \frac{\rho h_w}{(1 - \phi)} \frac{\partial \phi}{\partial t} \quad (2)$$

for the temperature field $T(x, z, t)$. Here, C_w and C_r are heat capacities of fluid and rock, respectively, ρ_r is density of the rock grains, K is thermal conductivity, and h_w is fluid enthalpy. A coupled solution to Eq. 1 with topographic relief specified as a boundary condition gives the ground-water discharge vector \mathbf{q} . A heat flux was supplied across the lower boundary to represent cooling of the earth's interior, and the top surface was held at constant temperature.

For the brines to reach the ore districts warm, they must have traveled through aquifers rapidly enough to have avoided cooling by conduction to the surface. Figure 5 shows formation temperatures of sphalerite (ZnS) from various districts in Arkansas, Missouri, Oklahoma, and Kansas (19). The sphalerite probably precipitated from brines migrating northward out of the Arkoma basin (20). The modes of the temperature data suggest that the ore-forming fluids cooled as they moved northward from the Arkoma basin at $\partial T/\partial x$ of about 0.1°C per kilometer. Balancing the heat carried laterally by ground waters with conductive loss to the surface gives the past ground-water discharge

$$q = \frac{K}{b\rho C_w} \frac{\partial T'/\partial z}{\partial T/\partial x} \quad (3)$$

where K is thermal conductivity of the overlying strata, b is thickness of the aquifer, and $\partial T'/\partial z$ is the geothermal gradient in excess of background. If it is assumed that flow occurred through the Lamotte sandstone, the most permeable regional aquifer, Eq. 3 predicts past discharge of tens of meters per year.

Small sedimentation rates characterize basins in continental interiors; rates in the Illinois and Arkoma basins averaged 0.03 and <0.5

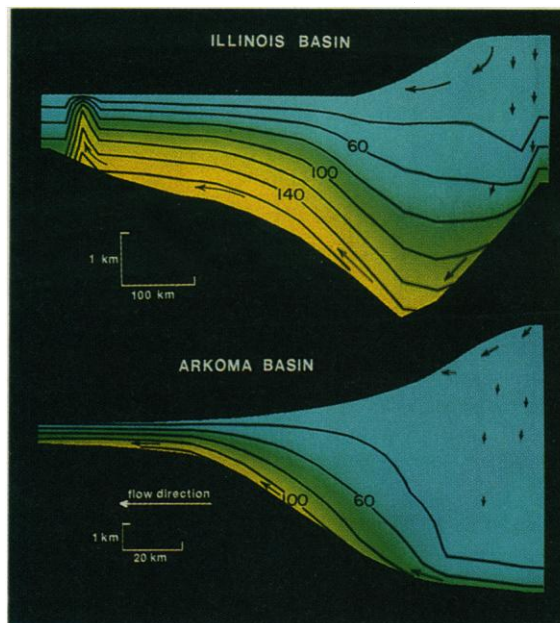


Fig. 6. Calculated temperature distributions (°C) in Illinois and Arkoma basins resulting from ground-water flow driven by topographic relief on the Pascola arch and Ouachita Mountains. Vertical exaggeration is 70:1 for the Illinois and 7:1 for the Arkoma basin.

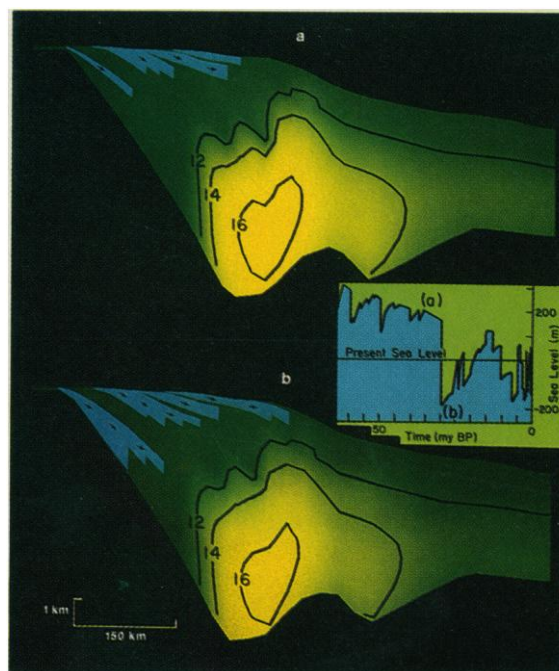


Fig. 7. Extent of basinward flow from relief on coastal plain (a) before and (b) after a drop in sea level 31 million years ago (blue areas). The interface between meteoric and compactional flow systems moves deeper and farther basinward in response to lowered sea level. Contours and color shading show pressure gradient (in megapascals per kilometer) in compactional regime.

mm/year, respectively. Our calculations (21) show that sediment compaction drove ground waters at velocities less than a few centimeters per year in the Illinois and Arkoma basins because of this slow burial. At such velocities ground waters could not have redistributed heat to the basin arches because they would have cooled by conduction. The calculations indicate that geopressures did not arise from compaction of the Illinois basin because of its slow burial and extensive aquifers, and that only small overpressured zones formed in the Arkoma basin. Decompressing geopressured zones is thus unlikely to have driven the migrations. Compression during continental collisions also cannot displace brines rapidly because plates move only centimeters per year.

Calculations accounting for the effects of past topography, however, show that warm fluids can be transported onto basin arches by flow systems that drain uplifted areas. Figure 6 shows calculated flow systems and temperature distributions that were caused in the Illinois basin from uplift of the Pascola arch and in the Arkoma basin from elevation of the ancient Ouachita Mountains. Some of the ground waters recharging in the uplifted areas move to depth and migrate along deep aquifers at velocities of meters to tens of meters per year. Migrating ground waters entrain heat that is conducted from the lower crust and redistribute it toward discharge areas. Temperatures, which in the absence of flow would increase linearly with depth, are depressed near the recharge areas and are significantly increased toward areas of discharge. By this process, warm ground waters move from deep basins into shallow sediments. A number of age determinations of diagenetic minerals precipitated from midcontinent brines match known ages of tectonic uplifts caused by continental collisions (20, 22). These results suggest that brine migrations occur as events related to tectonic uplift and indicate that the timings and pathways of past migrations can be predicted from the distribution of midcontinent aquifers and the theory of plate tectonics.

The inferred role of tectonic uplift in driving brine migrations has important implications for resource exploration. For example, the Michigan basin is broadly similar to the mineralized basins of the midcontinent except that it has not been subjected to uplift. This basin has been explored extensively for Mississippi Valley-type ores without success. Evidence of past uplifts is generally preserved in the geologic record; the elevated regions are exposed to erosion and become sources of sediment deposited in surrounding areas. This evidence should be used to refine exploration strategies. Petroleum is most likely to have been displaced from source rocks along migration paths emanating from uplifted areas. Exploration for metallic ores should be focused on arches that are located on the opposite sides of basins from areas that have undergone past uplift.

Freshwater Incursion

Shallow ground waters in basins with surfaces exposed above sea level are dilute meteoric (rain) waters, but underlying pore fluids are more saline. Salinity tends to increase with burial depth so that ground waters just a few hundred meters from the surface can be brines containing more than 10% dissolved solids by weight. Relatively fresh waters are sometimes found in strata several kilometers deep, however, and analyses of stable isotopes show that many deep brines are meteoric waters that have increased in salinity over time. In addition, diagenetic evidence indicates that dilute fluids have moved through deep aquifers that are filled with brines today.

Understanding the extent of freshwater incursion in the present and in the geologic past is important because of the chemical and physical changes the infiltrating waters cause in the subsurface. Silicate and sulfide minerals that are stable in sedimentary brines

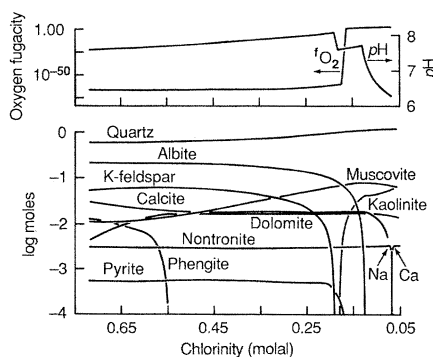


Fig. 8. Calculated reaction path (at 60°C) of meteoric water infiltrating a feldspathic sandstone. The sandstone is initially in equilibrium with a sedimentary brine.

dissolve in the dilute waters, creating potential reservoir rocks. Carbonate minerals precipitate as cements when bicarbonate ions in fresh waters react with minerals or cations in brines. Oxygen and microbes transported from the surface can degrade petroleum. Ores form when uranium and other elements leached in trace amounts from rocks near the surface become less soluble as ground waters move into reducing conditions. Fresh ground waters encountered during petroleum exploration can cause readings from well logging tools to be misinterpreted because both low-salinity water and oil have high electrical resistivities.

The Gulf Coast basin contains two principal hydrologic regimes: a meteoric system in which ground waters are driven basinward by the topographic relief of the coastal plain, and a deeper system in which saline brines migrate upward and landward in response to sediment compaction (23). The position of the interface between these systems depends on the amount of relief that drives the flow basinward, the pressures that are caused by compaction that counteract basinward flow, and the permeabilities of deep aquifers.

We modeled the interaction of freshwater and compactional flow systems in the Gulf Coast (4). Our calculations follow those applied to study geopressures (Eq. 1). In the calculations, the onshore top boundary condition describes elevation of the water table along the coastal plain. Figure 2 shows simulation results for the present day. Relief on the coastal plain drives fresh waters 1 to 2 km deep along Eocene, Oligocene, and Miocene aquifers. Flow extends for tens of kilometers into offshore strata. The calculated extent of the meteoric system agrees with observations of the salinity distribution of Gulf Coast ground waters (24).

Our calculations also show more extensive freshwater incursions occurring in the past as events that accompanied past drops in sea level. Figure 7 shows the calculated extent of the meteoric regime before and after a drop in sea level 31 million years ago. The drop increased topographic relief and exposed more of the coastal plain to meteoric precipitation at a time when overpressures from compaction were less intense than today. As a result, the meteoric regime extended deeper and farther basinward. These results agree with mineralogic and isotopic studies of diagenetic alteration that show greater past invasion of fresh waters in deep aquifers (25). Occurrence of freshwater incursions as events driven by changes in sea level suggests that the timing of freshwater diagenesis in compacting basins can be predicted from global sea level variations, which are known for much of geologic time (26).

Diagenetic Modeling

Diagenetic minerals record past temperatures and hydrologic regimes so that quantifying the relation of subsurface conditions to diagenesis helps to interpret basin histories. We simulate subsurface interactions by tracing the irreversible reaction paths (27) taken by

chemical systems open to mass fluxes. Figure 8 shows reaction of a sandstone typical of the Gulf basin with a meteoric ground water. The sandstone, containing quartz, albite, potassium feldspar, calcite, and pyrite, is buried 1 to 2 km and filled with a reducing, slightly alkaline brine. The meteoric water is dilute and charged with oxygen and carbon dioxide from the atmosphere and root zone.

Adding meteoric water to the sandstone dilutes the pore fluid and thus dissolves minerals that were stable in the original brine. Other minerals precipitate as cements. Phengite, a magnesium clay, dissolves early in the reaction and produces Mg^{2+} ions that react with calcite to produce dolomite. Dolomite cements are known to form where fresh and saline ground waters mix. The remaining calcite is consumed to produce a calcium clay. Further influx destabilizes feldspar by diluting cation concentrations and supplying carbon dioxide as carbonic acid. The dissolved feldspars precipitate as quartz, muscovite (a proxy for illite), and, after the potassium feldspar is consumed, kaolinite cements. Feldspar hydrolysis acts to increase the alkalinity of the fluid initially; but acid released as pyrite oxidizes and the continued supply of carbon dioxide eventually overwhelm the silicate reactions. After the feldspar has been consumed, pH decreases until acidity is buffered by reactions among carbonate species. Feldspar that has been altered to illite and kaolinite is commonly observed in permeable Gulf sediments that have probably been exposed to meteoric ground waters, such as those underlying major unconformities.

Feldspar hydrolysis and calcite dolomitization both increase pore volume in sediments by reducing mineral volume to create potential reservoir rocks. As the search for petroleum reaches deeper and less porous strata, quantitative analysis of diagenetic reactions will become increasingly important to understanding the distribution of reservoir rocks. Such calculations can also be applied to predicting the results of chemical treatments to stimulate recovery from oil wells and predicting the consequences of injecting toxic and radioactive wastes into deep strata.

Smectite Diagenesis

Smectite, a hydrated clay mineral common in sedimentary basins, transforms during burial to a dehydrated clay, illite (28). The reaction proceeds through a series of intermediate phases in which crystals are composed of smectite and illite layers. Each layer is about 1 nm thick. Initially, layers within the illite-smectite crystals fall into apparently random arrangements. As they react toward illite, the minerals develop a statistical ordering of their layers that is evident from low-angle peaks in x-ray diffraction patterns (29). Water released from smectite contributes to forming geopressures and helps drive petroleum from source rocks into reservoirs (30). Silica, magnesium, and iron produced by the reaction precipitate as cements in sandstones (31). Patterns of illitization in basins and the type of ordering attained give clues to thermal histories of sediments and the distribution of beds that are mature petroleum sources (32).

We studied the development of layer ordering in illite-smectite with a Monte Carlo numerical model (33), so named because it uses a random number generator to mimic stochastic processes. The reaction mechanism is poorly known, in part because of the difficulty of imaging illite-smectite by transmission electron microscopy. Some related minerals, however, transform (for example, biotite to chlorite) by reaction of individual layers (34). Our calculation models a layer-by-layer reaction in which the likelihood of smectite layers transforming to illite depends on interactions among neighboring layers. Thousands of one-dimensional crystallites composed of smectite layers are set up in the memory of a computer. The calculation randomly chooses smectites as candidates

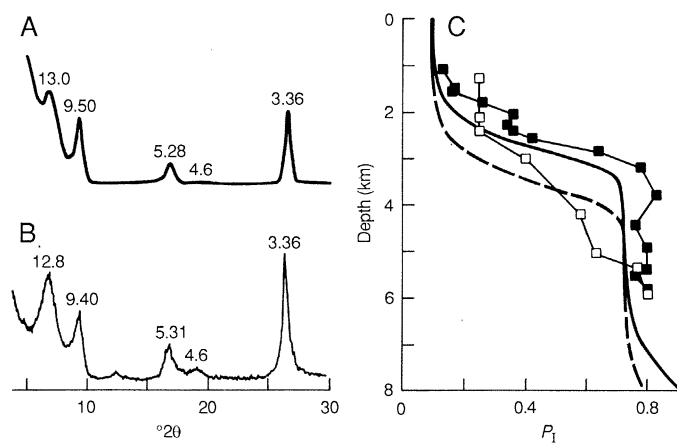


Fig. 9. Comparison of (A) calculated and (B) observed x-ray diffraction patterns. The calculated pattern assumes ordered interlayering with 70% illite layers; the observed pattern is from Cretaceous potassium-bentonite in the Montana disturbed belt. (C) Reaction profiles predicted by a Monte Carlo numerical model (bold solid and dashed lines) compared to observed reaction profiles (lines marked with squares) in the Gulf Coast basin. The bold solid line and the line with filled squares represent a burial rate of 0.2 mm/year; the dashed line and the line with open squares, 0.8 mm/year.

for reaction and then stochastically decides whether to transform the layer to illite. The probability of a candidate reacting depends on the types of neighboring layers. There are three possibilities: a candidate between two smectite layers, one illite and one smectite layer, or two illite layers.

We tested schemes for choosing reaction probabilities by calculating (35) the x-ray diffraction patterns that would be produced from the synthetic crystallites at various stages of illitization and comparing these to natural samples (Fig. 9, A and B). The natural reaction is best simulated when smectites with one illite neighbor are twice as likely to react as those with only smectite neighbors and are at least ten times more reactive than those with only illite neighbors.

By this scheme, packets of illite layers tend to grow within smectite domains because the smectite layers neighboring illite layers are the most reactive. Smectites between illites, however, react more slowly, so that illite packets are unlikely to merge until late in the reaction. This phenomenon of packet growth appears to produce the ordering observed by x-ray diffraction. Observations by others with an electron microscope indicate that small illite packets form and grow within a smectite matrix in suites of illite-smectite minerals (36), which supports the proposed reaction mechanism. In addition, images of dispersed illite-smectite (37) show layer packets several nanometers thick in distributions roughly matching the packet thicknesses predicted by Monte Carlo experiments.

Predicting the timing of illitization during basin development helps reconstruct the hydrologic and thermal histories of sediments. Reaction progress has been described as a function of time and temperature under a variety of thermal conditions by kinetic rate laws. First-order laws accurately describe the onset of illitization in basins. These laws take the form

$$\frac{dP_1}{dt} = (1 - P_1)k \quad (4)$$

where P_1 is the fraction of illite layers and the rate constant k varies exponentially with temperature. Such rate laws, however, predict illitization proceeding to completion at lower temperatures than observed in nature. The Monte Carlo modeling suggests that reaction rates depend on the neighbors of reacting layers. In this case, a first-order law is given by

$$\frac{1}{(1 - P_1)} \frac{dP_1}{dt} = X_0 k_0 + X_1 k_1 + X_2 k_2 \quad (5)$$

where X_i are the fractions of smectite layers with each of the three possible combinations of neighbors and k_i are the corresponding rate constants. Because the ratios among the constants k_i are given directly as results of the Monte Carlo experiments, this law can be evaluated with the same data as Eq. 4. Solutions $P_1(z)$ to Eq. 5 that assume a constant burial rate (Fig. 9C) follow the S-shaped profile commonly observed in basins (28, 38). The predictions of reaction progress in illite-rich strata that are based on such solutions are better than those formed on the basis of rate laws that do not account for interactions among layers.

Future Directions

Supercomputer analysis is unique in its ability to integrate data, sort among competing processes, maintain natural time and distance scales, and give integrated pictures of basin development. Through our experiments we sought a basic understanding of some of the dominant hydrologic and chemical processes operating in basins. The experiments, however, fall far short of integrating all of the dynamic aspects of basin evolution, or of representing details of the complexity of the subsurface.

Considering the vast sums of money spent annually on resource exploration worldwide, there is considerable impetus to further the development of quantitative techniques. We believe that more powerful computers, faster visualization devices, and improved numerical methods and databases will foster advances in computational analysis applied to geologic problems. Because the calculation techniques rely on the results of laboratory and field study, refined models will require increasingly detailed understandings of material properties and the mechanisms by which subsurface processes operate. Exploring calculation results parametrically will suggest which measurements are most significant. Thus, the numerical experiments will influence the directions of field and laboratory research. In addition, progress awaits conceptual advances in projecting the hydrologic and chemical properties that are observed on the time and distance dimensions of the petroleum reservoir or the laboratory to the scale of a sedimentary basin. Interdisciplinary effort will be required, for example, to find improved techniques of describing the regional-scale permeabilities of heterogeneous aquifer

and aquitard systems, the migration of hydrocarbon phases through composite media, and the kinetics of slow chemical reactions.

REFERENCES AND NOTES

1. D. J. Kuck, E. S. Davidson, D. H. Lawrie, A. H. Sameh, *Science* **231**, 967 (1986).
2. J. L. Pindell, *Tectonics* **4**, 1 (1985).
3. G. Dickinson, *Am. Assoc. Pet. Geol. Bull.* **37**, 410 (1953); C. M. Bethke, *J. Geophys. Res.* **91**, 6535 (1986).
4. W. J. Harrison and C. M. Bethke, *Geol. Soc. Am. Abstr. Programs* **18**, 630 (1986); C. M. Bethke and W. J. Harrison, *ibid.*, p. 540.
5. C. M. Bethke, *J. Geophys. Res.* **90**, 6817 (1985).
6. R. H. Wallace *et al.*, *U.S. Geol. Surv. Circ.* **790**, 132 (1979).
7. D. J. Timko and W. H. Fertl, *J. Pet. Technol.* **23**, 923 (1971).
8. P. R. Vail *et al.*, *Am. Assoc. Pet. Geol. Mem.* **26**, 49 (1977).
9. D. A. Sverjensky, *Annu. Rev. Earth Planet. Sci.* **14**, 177 (1986).
10. W. G. Dow, *Am. Assoc. Pet. Geol. Bull.* **58**, 1253 (1974).
11. J. L. Clayton and P. J. Swetland, *ibid.* **64**, 1613 (1980).
12. S. O. Moshier and D. W. Waples, *ibid.* **69**, 161 (1985).
13. C. M. Bethke, J. D. Pruitt, M. H. Barrows, *ibid.* **68**, 454 (1984).
14. J. Oliver, *Geology* **14**, 99 (1986).
15. S. A. Jackson and F. W. Beales, *Can. Soc. Pet. Geol. Bull.* **15**, 383 (1967).
16. J. M. Sharp, Jr., *Econ. Geol.* **73**, 1057 (1978).
17. G. Garven and R. A. Freeze, *Am. J. Sci.* **284**, 1085 (1984).
18. R. W. Dalrymple, G. M. Narbonne, L. Smith, *Geology* **13**, 607 (1985).
19. Data were compiled by E. L. Rowan from D. L. Leach, R. C. Nelson, and D. Williams [*Econ. Geol.* **70**, 1084 (1975)]; R. A. Schmidt [*ibid.* **57**, 1 (1962)]; J. C. Cobb [thesis, University of Illinois, Urbana-Champaign (1981)]; E. Roedder [*Econ. Geol.* **72**, 474 (1977)]; and D. L. Leach [*ibid.* **74**, 931 (1979)].
20. D. L. Leach and E. L. Rowan, *Geology* **14**, 931 (1986).
21. C. M. Bethke, *Econ. Geol.* **81**, 233 (1986); C. M. Bethke, *Geol. Soc. Am. Abstr. Programs* **18**, 540 (1986).
22. P. P. Hearn, Jr., and J. F. Sutter, *Science* **228**, 1529 (1985); ———, H. E. Belkin, *Geochim. Cosmochim. Acta* **51**, 1323 (1987).
23. W. E. Galloway, *Am. Assoc. Pet. Geol. Mem.* **37**, 3 (1984).
24. J. B. Wesselman, *U.S. Geol. Surv. Hydrol. Invest. Atlas* **HA-654** (1983).
25. R. S. Fisher, thesis, University of Texas at Austin (1982); P. D. Lundegard, thesis, University of Texas at Austin (1985); E. F. McBride, L. S. Laud, L. E. Mack, *Am. Assoc. Pet. Geol. Bull.* **71**, 1019 (1987).
26. B. U. Haq, J. Hardenbol, P. R. Vail, *Science* **235**, 1156 (1987).
27. H. C. Helgeson *et al.*, *Geochim. Cosmochim. Acta* **34**, 569 (1970).
28. E. Perry and J. Hower, *Clays Clay Miner.* **18**, 165 (1970).
29. R. C. Reynolds, Jr., and J. Hower, *ibid.*, p. 25; C. M. Bethke, N. Vergo, S. P. Altaner, *ibid.* **34**, 125 (1986).
30. J. F. Burst, *Am. Assoc. Pet. Geol. Bull.* **53**, 73 (1969).
31. J. R. Boles and S. G. Franks, *J. Sediment. Petrol.* **49**, 55 (1979).
32. J. Hoffman and J. Hower, *Soc. Econ. Paleontol. Mineral. Spec. Publ.* **26**, 55 (1979); P. H. Nadeau and R. C. Reynolds, *Clays Clay Miner.* **29**, 249 (1981).
33. C. M. Bethke and S. P. Altaner, *Clays Clay Miner.* **34**, 136 (1986).
34. D. R. Veblen and J. M. Ferry, *Am. Mineral.* **68**, 1160 (1983).
35. C. M. Bethke and R. C. Reynolds, *Clays Clay Miner.* **34**, 224 (1986).
36. J. H. Ahn and D. R. Peacor, *ibid.*, p. 165.
37. P. H. Nadeau, M. J. Wilson, W. J. McHardy, J. M. Tait, *Science* **225**, 923 (1984).
38. J. Hower, E. V. Eslinger, M. Hower, E. A. Perry, *Geol. Soc. Am. Bull.* **87**, 725 (1976).
39. Sponsored by National Science Foundation (EAR 85-52649 and EAR 86-01178), Amoco Production Company, Exxon Education Foundation, Shell Oil Company, Texaco USA, and Alliant Computer Systems, Inc. C. Norris, T. Corbet, and R. Idaszak helped make the calculations.